Glass Concrete Thin Sheets Prestressed with Aramid Fiber Mesh

Christian Meyer and Gregor Vilkner
Columbia University, New York, NY 10027, USA

Abstract

Concrete has been prestressed traditionally with high-strength steel. The vulnerability of such material to corrosion calls for alternate materials, if thin-sheet products are to be prestressed. A research project at Columbia University is investigating the feasibility of using aramid fiber mesh for such purpose. This paper explores the chemical and mechanical properties of aramid in the form of both individual fibers and rovings. Although the material is inherently brittle, its high strength and stiffness appear to make it a suitable medium for prestress applications. Appropriate pre-stretching of the mesh can minimize prestress losses due to relaxation. The low bond strength requires special measures for both stressing and anchoring of the mesh. Also the chemical interaction between the fibers and the cement matrix calls for attention. Because of the potential of crushed glass aggregate for decorative and architectural thin-sheet applications, pilot studies have been performed using glass concrete matrices.

1. Introduction

Prestressed concrete has traditionally been associated with high-strength steels to overcome the losses caused primarily by concrete creep. The requirement of protecting such steels against corrosion calls for minimum concrete covers, which dictate an overall thickness of at least 5 to 7 *cm* of any concrete member to be prestressed. For non-metallic reinforcement no such corrosion protection is needed, and thicknesses of a few *mm* are theoretically possible, limited primarily by the aggregate size. Woven fabrics or fiber mesh, also referred to as textile reinforcement, have proven to be a viable reinforcement medium. However, it has been reported in the literature that thin concrete covers are easily spalled off due to the curvature effect of such woven fabrics, when stressed as ordinary reinforcement [1]. If the fabrics are pretensioned, such curvature effects become negligible. Prestressing the embedded reinforcement, whether provided in the form of single rovings or continuous fiber mesh, greatly improves the mechanical properties of structural members and enhances their durability because of the absence of cracks. Also, delay of cracking creates sections with considerable strain capacities and flexibility.

Fax: (+1) 212 854 6267
E-mail: meyer@civil.columbia.edu

The substitution of crushed glass for natural aggregate opens up additional options, primarily in the field of decorative and architectural concrete, because of the esthetic potential of colored glass. But this is contingent on effective measures to counter the potentially damaging effects of alkali-silica reaction (ASR). At Columbia University, research efforts have been under way for a number of years to utilize waste glass as aggregate, and the work reported in this paper is a part of this ongoing larger effort.

Common performance requirements eliminate most of the fibers that are commercially available and in use in concrete applications. For the purposes of this study, only alkali-resistant (AR) glass, aramid, and carbon were considered. Because of their very high unit strengths, relatively low creep deformations, and high melting points, these materials are now being used mostly in fiber-reinforced plastics (FRP), e.g., for post-tensioning applications. All three materials are available in the form of woven or knitted fiber mesh, but exhibit highly linear elastic-brittle behavior, in contrast to metals.

Although AR-glass is popular as short fiber reinforcement, mainly to control shrinkage cracking, it has a lower static fatigue limit than aramid and carbon, relative to their respective ultimate strengths. Whereas carbon, because of its solid microstructure, is very stiff, aramid is flexible and fibrous, due to its polymeric nature. On small cross-sectional areas, carbon was found to be comparably difficult to handle. For these reasons, it was decided to focus on aramid as reinforcing material of choice for the studies reported herein. In the general public, aramid is best known as the basic material for body armor. The cost of aramid fiber mesh is still relatively high, however, manufacturers are steadily improving their production technologies. Once the resulting price reductions make new applications feasible, the increased demand for these materials can be expected to prompt further cost reductions due to the economy of scale.

2. Aramid fibers

2.1 Basic facts

The viscoelastic properties of polymer fibers are not at all comparable with those of classic reinforcing materials, such as steel. Developed by polymer chemists decades ago, these fibers have aroused the interest of civil engineers only in recent years. The transfer of knowledge between the two disciplines was slowed by the fact that polymer scientists have focused mostly on the behavior of single fibers with diameters of the order of 10 μm, whereas civil engineers are interested in load capacities that are usually about 6 orders of magnitude larger than the failure loads for a single fiber.

Aramids are a family of nylons including high-strength fibers known under trade names such as Kevlar, Twaron and Nomex. Aramid is a generic term applied to <u>ar</u>omatic poly<u>amid</u>es. A summary of aromatic high strength fibers has been compiled by Yang [2]. The basic molecular units are repeated to form polymer chains that connect to highly ordered crystallite structures. Such crystallites connect to fibrils that form the fibers. The chains align parallel to each other and connect via hydrogen bonds to form planar sheets. The

Fax: (+1) 212 854 6267
E-mail: meyer@civil.columbia.edu

sheets can stack, held together by Van der Waals forces, and build crystallites that are of considerable size. Figure 1 illustrates such a crystallite and a typical unit cell of which it is composed. With a size of the order of 5x25 *nm*, the crystallites are oriented along the direction of shear during flow. In an industrial spinning process, the polymer solution, also referred to as dope, is extruded through fine holes. During that operation the crystallites undergo significant reorientation. They can be regarded as domains that connect and form long fibrils that finally build actual continuous fibers with diameters of the order of 10 μm.

The fibrils and the crystallite domains they are made of are not oriented perfectly parallel to the fiber axis. Instead, orientation angles between domain and fiber axis of up to 20^o can be observed. Compared with the covalent bonds along the molecule chains, the bonding between the fibrils is not very strong. Also voids and other imperfections cannot be avoided. This is the reason for the fibrillar nature of aramid fibers. They can wear off on the outside or split. At the same time this also explains their toughness and the fact that they do not fail in as brittle a manner as glass or carbon fibers do [4].

DuPont developed the most popular of these fibers under the trade names Kevlar 29 and Kevlar 49 in 1966. Briefly afterwards, the AKZO Group developed aramid fibers in Europe under the trade name Twaron. In early 2001, the multi-national Teijin Corporation acquired Twaron Products and since then has been the producer of Twaron fibers and the third traditional aramid fiber, called Technora. In this study, Twaron fibers are used exclusively.

2.2 Mechanical behavior of fibers

The initial crystallite orientation is responsible for an individual fiber's initial uniaxial stiffness. As the fiber is stretched, e.g. in a strain-controlled experiment, two mechanisms determine the tangential stiffness and extent of deformation. For one, the crystallites stretch on the molecular chain level. The stiffness of the polymeric chain structure derives from the stiffness of the carbonyl and the amid bonds, as well as the stiffness of the phenylene rings. In one molecular chain these three components act in series. Within and between crystallites, hydrogen bonds between polymer chains and Van der Waals forces exist between planar arrangements of such polymer chains. Over longer distances, however, stresses are transferred between fibrils by shear forces. As long as there is no shear slip, the deformations are reversible and can be observed using Laser Raman Spectography [5]. The second important mechanism is the rearrangement of the crystallites towards the fiber axis. In a process, which can be characterized as yielding of polymers and is caused by rotational shear slip among crystallites, the highly ordered crystallites, which are not parallel to the fiber axis, start to rotate towards the fiber axis. This process is not reversible and can be experimentally detected by X-ray diffraction. For lower- modulus fibers, where this mechanism is more pronounced, a yield point can be identified between strain levels of 0.5% and 1%, beyond which such reorientation starts to take place.
Once these two basic deformational mechanisms are understood, the stress-strain behavior of aramid fibers in uniaxial tension can be explained, including phenomena observed

Fax: (+1) 212 854 6267
E-mail: meyer@civil.columbia.edu

during cyclic loading and long-term creep or relaxation deformations. Such tests are normally carried out on *rovings*, i.e., assemblies of thousands of fibers. The strengths of individual fibers are subject to some statistical distribution. In addition, not all fibers are loaded at the very beginning of a tension experiment. Finally, the low ductility of individual fibers and poor frictional shear between fibers cause a roving to fail at a load at which the fibers are stressed on average to about 70% of their capacity.

A nontrivial problem in fiber testing is how to stress a fiber without causing premature failure at the anchorage. Single fibers are usually fixed on paper, which is cut prior to the test and strengthened near the ends by epoxy glue. Gauge lengths range from 5*cm* to 50*cm*. It is well known, that the longer the fiber, the more likely failure will occur away from the ends. The strengthened fiber ends are usually held by mechanical clamps. Load cells must be very sensitive, since failure loads are usually below 50*gr*. Strain is preferably measured optically. Similar approaches can be used to test rovings, with special aluminum clamps to hold the rovings without the need for strengthening their ends with epoxy glue.

Single 1100 (low-modulus) and 2200 (high-modulus) den[*)] rovings failed at tensile loads of about 0.180*kN* and 0.450*kN*, respectively, and at ultimate strains between 2% and 2.5%, Fig. 2. Assuming these rovings to consist, respectively, of 1000 and 2000 circular fibers of 10μm diameter, the above failure loads correspond to ultimate strengths of 2.3*GPa* and 2.9*Gpa* and elastic moduli of 115*GPa* and 145*GPa*. The stress-strain curve of the low-modulus roving exhibits a yield point early in the loading process, followed by nonlinear response caused by the reordering of crystallites. The high-modulus roving response, on the other hand, is almost perfectly linear-elastic up to failure.

To investigate the response of a 2200 den Twaron roving to cyclic loading, a 0.222*kN* (50*lb*) load was applied. The corresponding strain was then held constant for 1*min* before unloading, and this load cycle was repeated. Subsequently, the load was increased by .044*kN* increments, with each load level applied twice. The load-deformation response depicted in Fig. 3 illustrates the permanent set caused by the change of the orientation distribution within single fibers. As predicted by the deformation mechanisms, the stiffness under the first loading is lowest and then increases during subsequent loadings to higher strain levels. At the same time, the first load cycle introduces a large permanent set, while subsequent load cycles increase it in smaller, but almost equal increments.

The previous experiment was repeated with an exactly reversed loading sequence, i.e. decreasing the load levels after two load cycles at a time. The different results can be seen in Fig. 4. Almost all permanent deformation is achieved in the first load cycle up to the highest load level, whereas subsequent cycles with lower strain levels introduce al-

---

[*)] In the fiber industry, Denier (den) denotes the weight in gram of 9000 m of a single fiber, while tex is the weight of 1000 m of a single fiber (i.e., 1 den = 9 tex)

Fax: (+1) 212 854 6267
E-mail: meyer@civil.columbia.edu

most no new permanent set. At the same time, the stiffness observed during the first load cycle is again lower than during the subsequent load cycles, during which it appears to remain about constant. This observation has important ramifications for the preconditioning of fibers for long-term loading, such as in prestress applications.

Creep and relaxation of aramid fibers have been studied with single fibers and fiber bundles, and a considerable body of knowledge exists [6-8]. The higher the fiber modulus, the lower the creep rate. Three different stages of creep behavior can be observed experimentally: primary, secondary and tertiary creep. Whereas secondary creep losses are recoverable, the much larger primary creep strains are not. During the third stage the rate of creep increases until failure occurs. The mechanisms responsible for the large primary creep are the same ones that were described in the previous section: as the crystallites rotate towards the fiber axis, the orientation distribution changes towards a more perfectly oriented fiber. Such reorientation can be deliberately forced by prestretching the fibers beyond the maximum strain to be experienced during the fiber's service life.

Numerous relaxation experiments were carried out during the course of this project to study the effect of fiber preconditioning. A typical result is shown in Fig. 5. A 2200 den Twaron roving was subjected to a load of .311*kN* (70*lb*), whereupon the corresponding strain was held constant for one minute, during which the load decreased from .311*kN* to .298*kN*. Next, the load was lowered to .267*kN*, which corresponded to a strain of about 60% of the failure strain. This strain was held constant for four hours, during which relaxation reduced the load from .267*kN* to .249*kN*. Finally, the roving was unloaded to .044*lb* and immediately reloaded to failure, which occurred at .533*kN*. The resulting load-deformation curve confirms the previously discussed deformation mechanisms. The stiffness of the roving during the second loading is clearly greater than that of the initial loading. Yet, after the preconditioning load level of .311*kN* is exceeded, the stiffness gradually decreases until it is similar to the one observed during the initial loading. In Fig. 6, the load vs. time response is plotted for the four-hour relaxation period. The resulting curve can be conveniently fitted by an exponential function, in this particular case with a relaxation coefficient of -0.014. Figure 7 summarizes the results of similar experiments with preconditioning load levels from zero to .178*kN* above the target load of .267*kN*. As expected, the higher the level of prestretching, the lower the relaxation rate. Moreover, the relaxation coefficient appears to be a linear function of the level of preconditioning.

2.3 Aramid fibers in alkaline environment

Like all aramid fibers, Twaron fibers have basically good chemical resistance, except in environments with extreme pH values. For this reason, fibers are often provided with protective coatings such as PVC, polyester or epoxy. Still, concerns do exist that the alkalinity of the pore solution in Portland cement paste can cause fibers to deteriorate. To investigate the effect of an alkaline solution, experiments were carried out, which are reported in detail elsewhere [9]. The observations made during those tests suggest that no cross-sectional area is lost due to deterioration caused by the alkaline solution. Instead,

Fax: (+1) 212 854 6267
E-mail: meyer@civil.columbia.edu

the alkaline solution can be interpreted as being a catalyst for fiber reorientation, weakening the secondary bonds between fibrils within single aramid fibers and therefore facilitating the rotation of crystallites towards the fiber axis. Yet, the impact of the pore solution in a Portland cement matrix can be expected to be different and is currently being studied.

3. Glass Concrete

Considerable progress has been made during recent years in the use of crushed consumer waste glass as aggregate for concrete and mortar. The susceptibility of glass to alkali-silica reaction (ASR) is well documented, yet, recent research has demonstrated that suitable countermeasures are available to suppress the damage that otherwise can be expected [10,11]. Thus it is possible to exploit the esthetic potential that colored glass aggregate offers for architectural and decorative applications [12]. Effects are possible that cannot be achieved with natural aggregates.

A number of criteria need to be considered when designing an appropriate glass concrete mix for prestressed thin sheets: optimum grading of the aggregate, upper bound of aggregate size (controlled by the fiber mesh dimensions), good workability and flowability, high early strength, as well as low creep deformations. The mix design proportions are summarized in Table 1. The compressive strength of the glass concrete mix after 24 hours was 32*MPa* (4.7*ksi*) and after 28 days 88.3*Mpa* (12.8*ksi*).

4. Glass concrete prestressed with aramid fiber mesh

The specimens used for preliminary studies were prismatic beams of 17.5*cm* (7*in*) length, 2.5*cm* (1*in*) width, and 7*mm* (1/4*in*) depth. A total of 7 layers of textile mesh, each with 5 rovings, was pretensioned with a total load of 2.2*kN* (500*lb*), which corresponds to about one-third of the total strain capacity (~3%) of the fibers. The total cross-sectional area of the aramid fibers was thus about 35,000 fibers @ $\pi/4\text{x}(10\mu m)^2 = 2.75 mm^2$, which amounts to a reinforcing ratio of 0.016.

After a period of trial and error it was decided to encase the ends of the fiber mesh layers in epoxy end blocks and to use mechanical clamps to simultaneously stress all seven layers of mesh. Figure 8 shows the end block and load cell used to monitor the amount of prestress. For formwork, standard hardware to produce 2.5x2.5x30cm^3 mortar bars was modified, making it possible to vary the concrete cover. Such variable cover may be necessary to accomplish different exposed aggregate surfaces for their architectural effect. At the same time, it permits to vary the prestress eccentricity. The prestress itself was applied by tightening regular nuts located just outside the two load cells. Further details of the experimental setup are found in [9]. It should be noted that Reinhardt and his co-workers [13] used a different experimental setup to achieve a similar purpose.

Fax: (+1) 212 854 6267
E-mail: meyer@civil.columbia.edu

Before stressing the fibers, they were preconditioned as described in the previous section, to “straighten them out”, with the result of greatly reduced subsequent losses due to relaxation. A mortar mix of the exceptionally high flow of 130mm was needed to assure that no voids were created and that it completely encased all 35 rovings in the five layers with only 0.75*mm* clear spacing in between.

As the work described herein is still in progress, only preliminary results can be presented here. These reflect some problems that need to be corrected or accounted for in subsequent tests. For example, it was observed during the production of some specimens, that about 10% of the initial prestress was lost within the first few hours of hydration, presumably as a result of alkali attack. On the other hand, this prestress loss appeared to stabilize quickly, probably because the glass concrete mix was designed to react very intensely during the first few hours, to engage as many hydroxide ions as possible in reacting with the powder admixture. There seems to have been no premature failure of a complete roving. The alkali ions may weaken the amid groups in the polymer molecules, but do not lead to complete failure of fibers.

After transfer of the 2.22*kN* (500*lb*) prestress load to the beam specimens, they were subjected to three-point bending. A representative load-deformation curve is shown in Fig. 9, and Fig. 10 illustrates the beam at maximum load and after unloading. During initial peak loading, a 1*mm* wide crack opened on the bottom face, and the compression zone experienced partial crushing failure. Yet, after unloading, the specimen returned to its initial shape, and the crack closed almost completely. The initial loading and unloading was followed by several cycles between CMOD of 0 and 1*mm*.

After these bending tests, the epoxy end blocks were removed using a diamond saw, and the three-point bending tests resumed. As expected, the fibers slipped, and as a result, the section’s capacity was reduced, and the crack did no longer close upon unloading, Fig. 11. It should be pointed out that the poor bond characteristics of aramid fibers pose probably the main challenge when using them for prestressing. Although the cement matrix can be expected to develop a limited bond with the fibers on the roving periphery, relatively little shear transfer is likely between those fibers and the ones situated within the interior of a roving. (Even in the end blocks, produced with the much more liquid epoxy, it is unlikely that all fibers are forced to contribute to the load capacity of a roving.) Thus, the rovings can be considered like unbonded tendons. With the removal of the end blocks, the prestressed fibers lose much of their effectiveness.

5. Conclusions

The knowledge of aramid fibers and their behavior gained from this study can be summarized as follows.

1. Deformation mechanisms of highly orientated aramid fibers are well understood in the polymer research community. Numerical models can successfully explain the time- and

Fax: (+1) 212 854 6267
E-mail: meyer@civil.columbia.edu

strain-dependent mechanical performance of such fibers. These mechanisms include a reversible linear-elastic stretching of the molecular chains and an irreversible reorientation of crystallites towards the fiber axis. This second mechanism is strain- dependent and therefore can be removed almost completely for consecutive loadings by prestretching the fibers to a level just below ultimate strength.

2. High-modulus fibers respond to tension almost linear-elastically up to fibrillar failure. Thus, if properly preconditioned and especially when considering rovings with several thousand fibers, perfectly linear-elastic behavior can be assumed together with a higher stiffness than that of low-modulus fibers.

3. The time-dependent fiber behavior is controlled by primary and considerably lower secondary creep strains. Again, if properly preconditioned, primary creep losses due to relaxation can be all but avoided for subsequent loadings. The secondary creep or relaxation is conveniently described by a logarithmic decay function with a single creep or relaxation coefficient.

4. Aramid fibers are chemically highly inert. But stressed fibers, in contact with concentrated NaOH solution, will ultimately lose considerable amounts of prestress, not so much due to degradation, but rather because of weakened secondary bonds between fibrils within single fibers. The performance of prestressed aramid fibers in a Portland cement based glass concrete matrix still remains to be investigated.

5. The low capacity of shear transfer between individual fibers and in particular the relatively low bond strength between aramid fibers and a cement-based matrix, pose the main practical challenges when aramid fiber mesh is considered for prestressing thin-sheet concrete products.

6. References

1. Curbach, M. et al, “Textilbewehrter Beton für die Verstärkung von Bauwerken”, Beton **8 (**2001), 430-434.
2. Yang, H.H., “Aromatic high strength fibers”, John Wiley, New York, 1989.
3. Dobb, M.G. and McIntyre, J.E., “Properties and applications of liquid crystalline main chain polymers”, Advances in Polymer Science, **60/61 (**1984), 61-98.
4. Pigliacampi, “Organic Fibers”, in *ASM Handbook*, Vol. 21, Composites. ASM International, 2001.
5. Yeh and Young, “Molecular deformation processes in aromatic high modulus polymer fibres”, Polymer **40** (1998), 857-870.
6. Baltussen, J.J.M. and Northolt, M.G., “The viscoelastic extension of polymer fibres: creep behavior”, Polymer **42** (2001), 3835-3846.
7. Ericksen,R.H., “Creep of aromatic polyamide fibres”, Polymer, **26** (1985), 733-746.
8. Guimaraes, G.B. and Burgoyne, C.J., “Creep behaviour of a parallel-lay aramid rope”, Journal of Materials Science, **27** (1992), 2473-2489.

Fax: (+1) 212 854 6267
E-mail: meyer@civil.columbia.edu

9. Vilkner, G., “Glass Concrete Thin Sheets Prestressed with Fiber Mesh”, Ph.D. Dissertation, Columbia University, in preparation, 2003.
10. Jin, W., “Alkali-Silica Reaction in Concrete with Glass Aggregate – A Chemo-Physico-Mechanical Approach”, Ph.D. Dissertation, Columbia University, 1998.
11. Jin, W., C. Meyer and S. Baxter, “Glascrete – Concrete with Glass Aggregate”, ACI Materials Journal, March-April 2000.
12. Meyer, C., “Cracking an ASR Barrier”, The Concrete Producer, April 2001.
13. Krüger, M., H.-W. Reinhardt and M. Fichtlscherer, “Bond behavior of textile reinforcement in reinforced and prestressed concrete”, Otto Graf Journal, Universität Stuttgart, Vol. 12, 2001.

Table 1. Glass Concrete Mix Properties

Material	Parts
Crushed Glass	172
Blue Circle Type III Cement Cementitious Admixture	80 20
Water	35
Superplasticizer	1.25

Glass Aggregate Grading

Sieve Size	#4	# 8	# 16	# 30	# 50	# 100
Fraction (% weight)	7	19	27	28	13	6

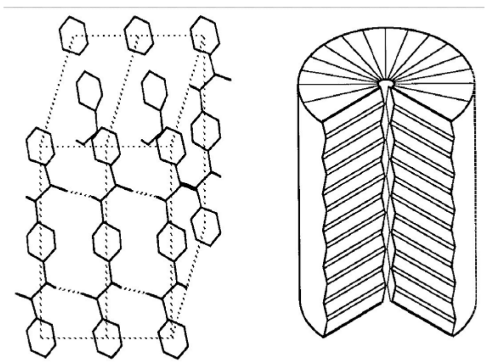

Fig. 1 Aramid Unit Cell and Crystallite [3]

Fax: (+1) 212 854 6267
E-mail: meyer@civil.columbia.edu

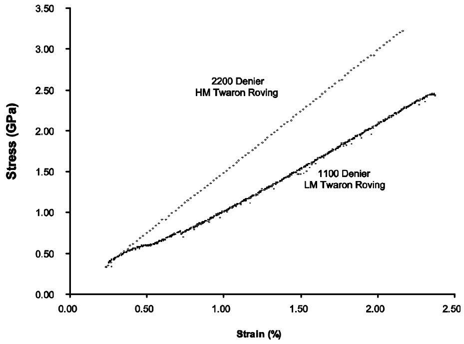

Fig. 2 Stress-Strain Diagrams of 1100 den Low-Modulus and 2200 den High-Modulus Single Rovings

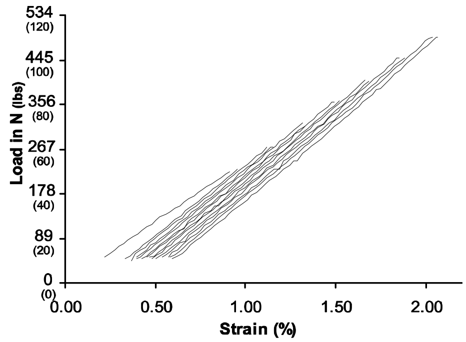

Fig. 3 Response of Single Roving to Repeated Loading of Increasing Amplitude (unloading branches not shown)

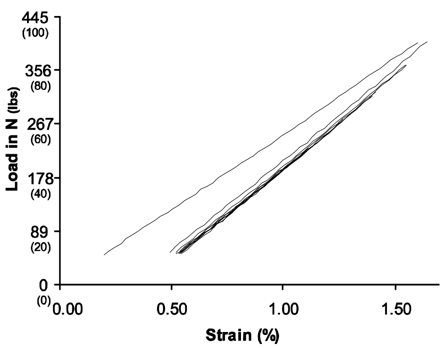

Fig. 4 Response of Single Roving to Repeated Loading of Decreasing Amplitude (unloading branches not shown)

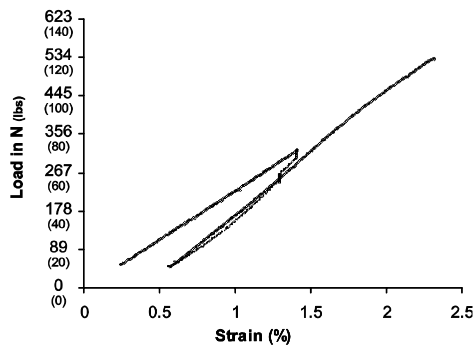

Fig. 5 Typical Load-Deformation Behavior with 10*lbs* Overstretch

Fax: (+1) 212 854 6267
E-mail: meyer@civil.columbia.edu

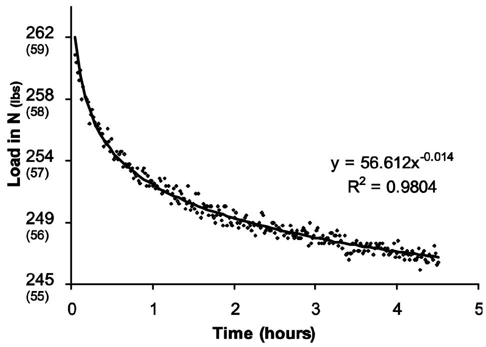

Fig. 6 Typical Relaxation Time History (10*lbs* Overload)

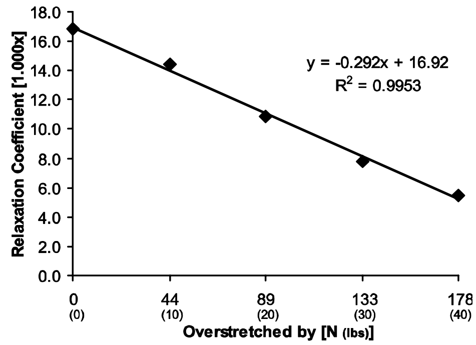

Fig. 7 Relaxation Coefficient vs Amount of Overload

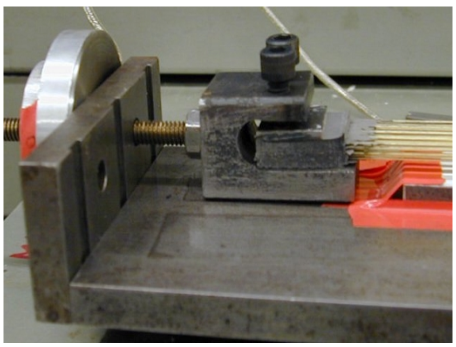

Fig. 8 End Block and Clamp Assembly

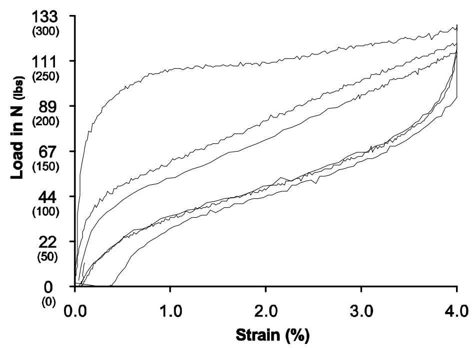

Fig. 9 Load-Strain Diagram for Typical Three-Point Bending Test (with End Blocks)

Fax: (+1) 212 854 6267
E-mail: meyer@civil.columbia.edu

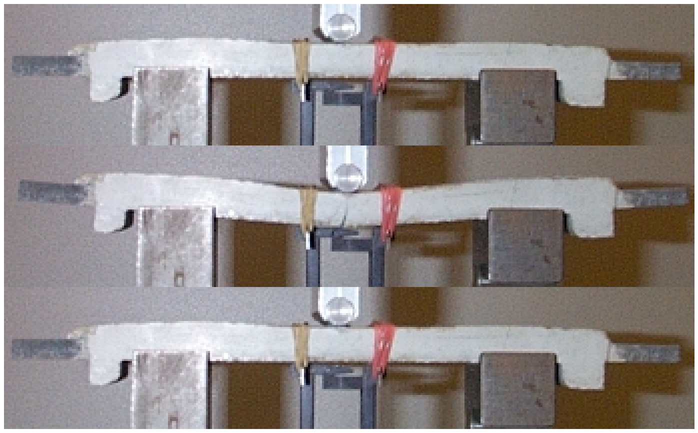

Fig. 10 Three-Point Bending Test of Specimen with End Blocks

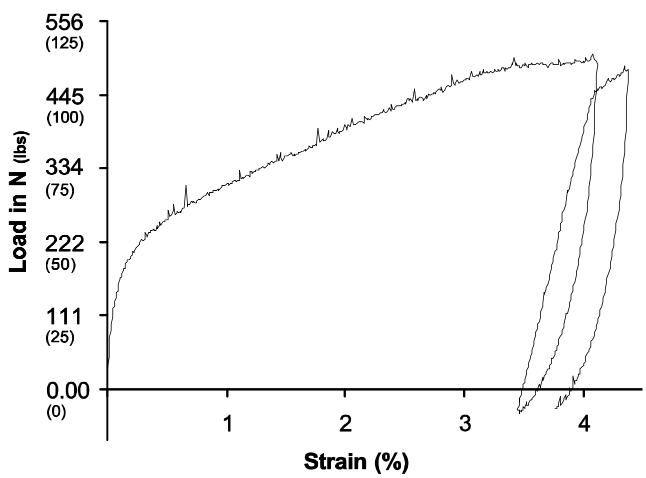

Fig. 11 Typical Load-Deformation Response for Three-Point Bending Test With End Blocks Removed

Fax: (+1) 212 854 6267
E-mail: meyer@civil.columbia.edu